The Specificity in the Interaction between Cytochrome *f* and Plastocyanin from the Cyanobacterium *Nostoc* sp. PCC 7119 Is Mainly Determined by the Copper Protein†

Cristina Albarrán, José A. Navarro, Miguel A. De la Rosa, and Manuel Hervás*

Instituto de Bioquímica Vegetal y Fotosíntesis, Centro de Investigaciones Científicas Isla de la Cartuja, Universidad de Sevilla y Consejo Superior de Investigaciones Científicas, Sevilla, Spain

Received October 5, 2006; Revised Manuscript Received November 20, 2006

ABSTRACT: The plastocyanin−cytochrome *f* complex from *Nostoc* exhibits relevant structural differences when compared with the homologous complexes from other cyanobacteria and plants, with electrostatic and hydrophobic interactions being differently involved in each case. Here, five negatively charged residues of a recombinant form of cytochrome *f* from *Nostoc* have been replaced with either neutral or positively charged residues, and the effects of mutations on the kinetics of electron transfer to wild-type and mutant forms of plastocyanin have been measured by laser flash absorption spectroscopy. Cytochrome *f* mutants with some negative charges replaced with neutral residues exhibit an apparent electron transfer rate constant with wild-type plastocyanin similar to or slightly higher than that of the wild-type species, whereas the mutants with negative charges replaced with positive residues exhibit a significantly lower reactivity. Taken together, these results indicate that the effects of neutralizing residues at the electrostatically charged patch of cytochrome *f* are smaller than those previously observed for mutants of plastocyanin, thus suggesting that it is the copper protein which determines the specificity of the electrostatic interaction with the heme protein. Moreover, cross reactions between mutants of both proteins reveal the presence of some short-range specific electrostatic interactions. Our findings also make evident the fact that in *Nostoc* the main contribution to the electrostatic nature of the complex is provided by the small domain of cytochrome *f*.

In oxygen-evolving photosynthetic organisms, cytochrome c_6 and plastocyanin (Pc)[1] are involved in the electron transfer from the cytochrome b_6f complex to photosystem I (PSI) (*1*−*3*). Cytochrome *f* (C*f*) is one of the redox components of the cytochrome b_6f complex and represents an atypical *c*-type cytochrome because of both its β-sheet secondary structure and the unusual heme axial coordination (*4*−*7*). It is an integral component of the membrane complex, with a hydrophobic α-helical tail of 35 residues which allows the correct orientation of the heme to connect both with the Rieske protein on the membrane plane and with the soluble acceptor on the luminal side (*8*). The soluble truncated form of the protein from different sources has been used with success to perform both structural and functional in vitro studies (*1*, *5*−*9*).

By its turn, Pc is a small (10.5 kDa) type I cupredoxin in which the copper metal is coordinated by two histidines, one methionine, and one cysteine (*1*, *2*). Two functional regions have been identified at the Pc surface: a hydrophobic area at the north pole of the molecule (the so-called site 1), which is involved in electron transfer, and an electrostatic patch in the east region (the so-called site 2), which is responsible for electrostatic interactions with its redox partners (*1*−*4*).

Both C*f* and Pc are structurally well conserved among plants, algae, and cyanobacteria except for the electrostatic properties at the surface level. A well-conserved positively charged ridge is present in plant and algal C*f*, but the surface electrostatic potential of this area is negative in cyanobacteria. In any case, Pc and C*f* possess just contrary electrostatic charges on their respective electrostatic patches, thereby making the electrostatic interactions between them both attractive in all cases (*1*, *5*−*9*).

Extensive kinetic and structural analyses of the transient Pc−C*f* complex have been carried out in a variety of organisms, with relevant differences being observed with regard to the reaction mechanism and relative orientation of the two partners inside the complex (*10*−*18*). First, the redox interaction is mainly hydrophobic in the cyanobacterium *Phormidium laminosum* (*13*, *19*) but electrostatically driven in plants (*8*). Second, Pc binds to C*f* in a "head-on" conformation in *Phormidium*, in which the hydrophobic patch of Pc accounts for the whole recognition interface area, but

† This work was supported by grants from the European Commission (HPRN-CT1999-00095), the Spanish Ministry of Education and Science (AP2001-1256 and BMC2003-00458), and the Andalusian Government (PAI, CVI-0198).

* To whom correspondence should be addressed: Instituto de Bioquímica Vegetal y Fotosíntesis, Universidad de Sevilla y CSIC, Américo Vespucio 49, 41092 Sevilla, Spain. Telephone: 34-954-489-514. Fax: 34-954-460-065. E-mail: mhervas@us.es.

[1] Abbreviations: C*f*, cytochrome *f*; dRf, 5-deazariboflavin; k_2, second-order rate constant; K_A, equilibrium constant for complex formation; k'_{et}, apparent electron transfer rate constant; k_{obs}, observed pseudo-first-order rate constant; Pc, plastocyanin; PDQ, propylendiquat; PSI, photosystem I; WT, wild-type.

10.1021/bi0620757 CCC: $37.00
Published on Web 01/06/2007

in a "side-on" orientation in plants, with the acidic patch of Pc being involved as well (see ref *14* for a recent review).

Pc and C*f* from the cyanobacterium *Nostoc* sp. PCC 7119, in particular, represent an excellent case study as they react with each other by means of attractive electrostatic interactions, like plant and algal proteins (*20*), but using differently charged patches (positive in Pc and negative in C*f*). At low ionic strengths, the kinetics for C*f* oxidation by wild-type (WT) Pc are faster in *Nostoc* than in other organisms; however, the electron transfer rate in the *Nostoc* system is highly dependent on ionic strength (*21*), in contrast to the weak salt dependence previously described for the *Phormidium* system (*10*). Furthermore, the experimental data concerning *Nostoc* C*f*(WT) and Pc mutants (*21*) matched well the kinetic behavior exhibited by the same set of Pc mutants when they act as donors of electrons to PSI (*22*), thus indicating that the copper protein uses the same surface areas (one hydrophobic and the other electrostatic) to interact with both redox partners.

Interestingly, the three-dimensional structure of the *Nostoc* Pc−C*f* complex has been recently characterized by NMR spectroscopy (*17*), thus revealing that this complex adopts a peculiar conformation which is between the plant side-on and the *Phormidium* head-on orientation (*23*). However, the interaction of the *Nostoc* complex involves both the hydrophobic and electrostatic patches of both proteins, as is the case in plants (*16*, *17*, *23*). From the structure of this complex, some residues of C*f* have been identified as being involved in binding to Pc, namely, residues D100, E108, and E165 at the hydrophobic patch and residues D64 and E189 at the electrostatic site (*17*).

Here we report a laser flash-induced kinetic analysis of the oxidation of site-directed mutants of *Nostoc* sp. PCC 7119 C*f* by WT Pc and a set of mutants of the copper protein previously analyzed with C*f*(WT) and PSI (*21*, *22*), thereby providing relevant information about the role played by the modified residues on the interaction between the two redox partners. These findings are discussed in the light of the recently determined structure of the *Nostoc* Pc−C*f* complex.

EXPERIMENTAL PROCEDURES

Mutagenesis of the petA Gene. The molecular biology methods that were used were essentially as described in ref *24*. The plasmid encoding C*f*(WT) (pEAFwt) was obtained as described in ref *21*. Mutagenesis of the *petA* gene in the pEAFwt vector was carried out with the Stratagene QuickChange mutagenesis kit according to the manufacturer's instructions. To obtain the different mutants, oligonucleotides of 21 bp with the following codon changes were used: GAT to GCT for D64A and D100A, GAA to GCA for E108A, E165A, and E189A, GAT to AAG for D64K and D100K, and GAA to AAA for E108K, E165K, and E189K. Incorporation of the desired mutations and the absence of additional changes were checked by sequencing the mutated constructs.

Expression, Purification, and Characterization of Cf and Pc Variants. Expression, purification, and characterization of WT and mutant C*f* were carried out as described in ref *21*, with minor modifications. Protein expression was optimized by growing *Escherichia coli* cells at 37 °C for 48 h with 100 rpm stirring; under these conditions, the yield of C*f*(WT) was increased up to 3 mg/L, although this figure varied depending of the mutant. The yield was somewhat higher for mutants E108A, E108K, E165A, E189A, and E189K and markedly lower for the double mutants.

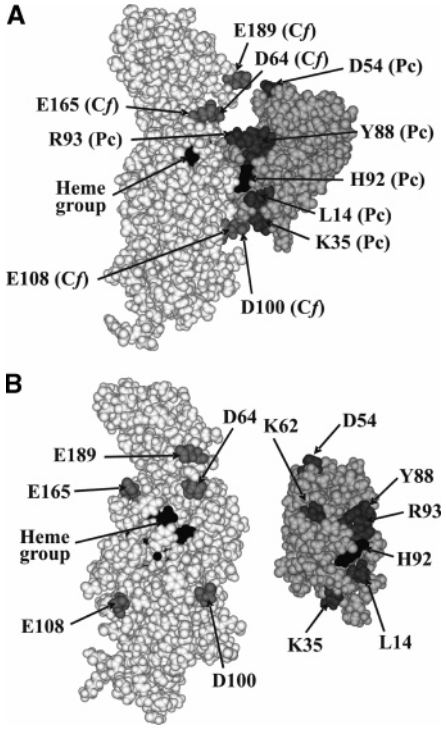

FIGURE 1: (A) Space-filling model of the *Nostoc* Pc−C*f* complex (*17*) showing the residues of the heme and copper proteins modified by site-directed mutagenesis. C*f* is depicted in light gray, whereas Pc is colored dark gray. The heme group of C*f* and the Cu ligand His92 of Pc are colored black. (B) Pc and C*f* are rotated 90° to the right and to the left, respectively, with respect to their orientation in the complex to show their interaction areas.

The proteins were purified essentially as described in ref *21*. The purity of the isolated C*f* variants was inferred from the A_{275}/A_{556} ratio of the reduced protein; protein preparations with a ratio lower than 1.5 were used for the kinetic analyses. The redox potential of mutant proteins was determined as previously described (*21*).

Pc WT and its mutants were produced and purified as described in refs *21* and *22*.

Laser Flash Absorption Spectroscopy. Laser flash experiments were carried out essentially as described in ref *21*, by producing submicromolar amounts of reduced C*f* with the dRf/PDQ^+ system to trigger the interprotein redox reaction. Protein concentrations were determined using the following absorption coefficients: $\epsilon_{556} = 31.8\ mM^{-1}\ cm^{-1}$ (*21*) and $\epsilon_{597} = 4.5\ mM^{-1}\ cm^{-1}$ (*22*) for reduced C*f* and oxidized Pc, respectively. The concentration of oxidized C*f* in the reaction cell was 50 μM for all the mutants except D64K and D64A/E189A, for which the concentration in the cuvette was decreased to 40 μM to prevent protein aggregation.

RESULTS AND DISCUSSION

The three-dimensional structure of the *Nostoc* Pc−C*f* complex has recently been characterized by NMR spectroscopy (Figure 1) (*17*). A precise analysis of the interface area of the complex makes evident the fact that five acidic residues on the heme protein seem to play a relevant role in the electrostatic interactions with positive groups of the

Table 1: Values for the Apparent Electron Transfer Rate Constant (k'_{et}) for the Oxidation of C*f* Variants, with Single or Double Mutations to Alanine, by WT and Mutant Pc[a]

	WT Pc	L14A Pc	K35A Pc	D54K Pc	K62A Pc
C*f*(WT)[b] (+334)	13400	7300	5200	25500	7000
C*f*(D64A) (+338)	13300				4600
C*f*(D100A) (+337)	17700	7000	5000		
C*f*(E108A) (+336)	14500				
C*f*(E165A) (+344)	19500				5900
C*f*(E189A) (+337)	13600			16600	
C*f*(D64A/E189A) (+331)	12000			13900	5800
C*f*(D100A/E108A) (+334)	10800	7300[c]	6400		

[a] The units for k'_{et} values are inverse seconds. The K_A value was estimated using the method of Meyer et al. (*26*). The redox potential value for each mutant (expressed in millivolts, at pH 7.0) is in parentheses. [b] Data from Albarrán et al. (*21*). [c] $K_A = 3.4 \times 10^6$ M^{-1}.

Table 2: Values for the Apparent Electron Transfer Rate Constant (k'_{et}) for the Oxidation of C*f* Variants, with Single Mutations to Lysine, by WT and Mutant Pc[a]

	WT Pc	K35E Pc	D54K Pc	K62E Pc	Y88F Pc	R93E Pc
C*f*(WT)[b] (+334)	13400	3800[c]	25500	2300	13400	1800[d]
C*f*(D64K) (+336)	7500			5000		
C*f*(D100K) (+336)	8600	2100				
C*f*(E108K) (+332)	8500	1800				
C*f*(E165K) (+338)	7000			1800	7800	1200
C*f*(E189K) (+333)	8300		12600	2100		

[a] The units for k'_{et} values are inverse seconds. The K_A values were estimated according to the method of Meyer et al. (*26*). The redox potential value for each mutant (expressed in millivolts, at pH 7.0) is in parentheses. [b] Data from Albarrán et al. (*21*). [c] $K_A = 10^5$ M^{-1}. [d] $K_A = 10^6$ M^{-1}.

copper protein. Figure 1 shows the location of these five residues in the structure of C*f*: Asp64 and Glu189, located at the small domain of the heme protein, which contains the acidic ridge; Asp100 and Glu108, which are at the large domain; and Glu165, located near the hydrophobic patch of C*f* (Figure 1B). To investigate the relative contribution of these residues to the overall electrostatic interaction surface and to identify specific short-range electrostatic interactions between charge residues, a series of site-directed mutants that either neutralize their charge with a standard replacement with alanine (*25*) or revert it upon replacement with lysine have been constructed. Two double alanine mutants, one concerning the two acidic residues of the small domain and the other concerning the two amino acids of the large domain, have also been made. The reactivity of all these C*f* variants with WT and mutant forms of Pc has been analyzed by laser flash absorption spectroscopy.

The visible spectra of the different C*f* mutants, both in the oxidized and in the reduced states, were similar to those of the WT protein, and the molecular masses of purified proteins determined by MALDI-TOF spectroscopy were in agreement with the values predicted from the protein sequence (data not shown). None of the redox midpoint potential values of the C*f* mutants differed significantly from that of the WT species (Tables 1 and 2). All these results indicate that the global structure of the protein and the heme environment are not significantly altered in the mutants with respect to C*f*(WT). Moreover, the reactivity of all the mutants with PDQ was similar to that of the WT protein, ensuring a similar extent of reduced C*f* generated by the laser flash.

The kinetic profile of the reduction of WT and mutant Pc by the heme protein under standard conditions was monoexponential with all C*f* mutants (not shown), which was the case for C*f*(WT) (*21*), but the kinetic efficiency of the heme protein oxidation by Pc and the corresponding rate constants varied greatly (Figure 2 and Tables 1 and 2). As was the case with C*f*(WT), only a partial extent of protein oxidation was observed for all the heme protein mutants (not shown), a fact that can be attributed to the similarity of the redox potentials of C*f* and Pc, thus allowing a reversible electron transfer reaction up to the equilibrium according to the following scheme (*26*):

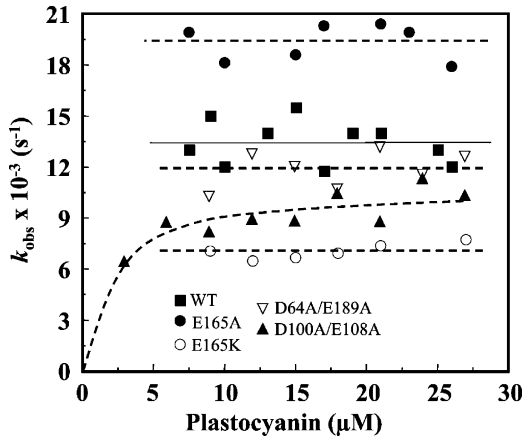

FIGURE 2: Dependence upon Pc concentration of k_{obs} for the oxidation of WT and some mutant species of C*f* by WT Pc. The dashed line for the D100A/E108A mutant corresponds to the theoretical fitting using the formalism in ref *26*. Experimental conditions were as described in Experimental Procedures.

$$Cf_{red} + Pc_{ox} \overset{K_A}{\rightleftharpoons} [Cf_{red} \cdots Pc_{ox}] \underset{k_{et\ reverse}}{\overset{k_{et\ forward}}{\rightleftharpoons}} Cf_{ox} + Pc_{red}$$

where K_A stands for the protein−protein association constant and $k_{et\ forward}$ and $k_{et\ reverse}$ stand for the reversible electron transfer rates. The two latter constants could correspond to regular rate constants but could also reflect an additional intracomplex rearrangement step prior to the electron transfer (*1*, *2*). The k_{obs} values for the oxidation of the alanine single mutants of C*f* by WT Pc were independent of Pc concentration within the range that was analyzed, as shown in Figure 2 for the C*f*(E165A) mutant. This indicates that all these mutants, as was the case for the WT protein (*21*), maintain a high association constant ($K_A \geq 10^6$ M^{-1}). From the data obtained in these reactions with WT Pc, an apparent first-order intracomplex forward electron transfer rate constant (k'_{et}) can be estimated (Table 1) (*21*). These estimated values were close to that of WT for all the alanine single mutants. The effects of C*f* mutations on k'_{et} are thus significantly smaller than those obtained for the reaction of a series of comparable charge mutants of Pc with C*f*(WT) (*21*). Whereas most of the mutants present k'_{et} values similar to that of C*f*(WT), the C*f*(D100A) and C*f*(E165A) variants exhibited an increased reactivity (Table 1), the highest k'_{et} value being obtained for the C*f*(E165A) mutant, in which the mutation is located near the heme group. In the WT Pc−C*f* complex, the residue at position 165 of C*f* is close (9 Å distance) to R93 of Pc (Figure 1) (*17*), a residue that has been shown to be crucial for the interaction of Pc both with PSI and with C*f* (*21*, *22*). This fact indicates that the weakening of the electrostatic interaction in the heme area promoted by the E165A replacement could affect the rearrangement of the

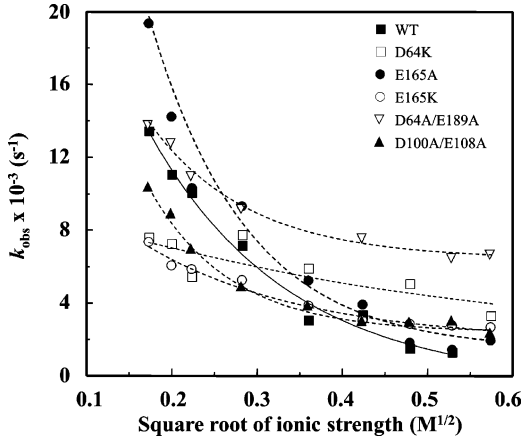

FIGURE 3: Ionic strength dependence of k_{obs} for the oxidation of WT and mutant species of C*f* by Pc. The Pc concentration was 24 μM. The solid and dashed lines are for the fitting of experimental data to the equation by Watkins et al. (*27*). Other conditions were as described in Experimental Procedures.

transient complex, thus allowing reorientation of the partners toward a more favorable configuration for electron transfer. Although this mutant is slightly more reductive than WT, the small difference in redox potential (ca. 10 mV, Table 1) alone could not account for the higher observed reactivity. However, the difference in the driving force for the interaction of this mutant with Pc is slightly reflected in the somewhat higher extent of C*f* oxidation by the copper protein with respect to WT (not shown). With kinetic behavior similar to that of the C*f*(E165A) variant, the C*f*(D100A) mutant is also located in a hydrophobic environment but could still exhibit a remarkable electrostatic character. Thus, the removal of this negative charge could also facilitate the rearrangement of the transient complex, improving the electron transfer. As a general conclusion for all the mutants showing an effect on k'_{et} and not on K_A, we cannot discriminate between an effect exerted on the electron transfer step itself and that exerted on the intracomplex rearrangement step prior to electron transfer, a very subtle process that can be altered by the different mutations.

It is interesting to note that the removal of the negative charge of D64 in *Nostoc* C*f* and its equivalent residue D63 in the *Phormidium* protein does affect quite differently the intracomplex electron transfer rate (*18*, *23*). The *Nostoc* C*f*(D64A) mutant exhibits a k'_{et} value similar to that of C*f*(WT), whereas the *Phormidium* C*f*(D63A) mutant is much less reactive (Table 1) (*19*). This result is as expected from the very different position of this residue in both complexes: in *Phormidium*, D63 is very close to and specifically interacts with the crucial R93 residue in Pc, whereas in the *Nostoc* Pc−C*f* complex, the two residues are 16.8 Å from each other (Figure 1A) (*23*).

To analyze the different role of charged groups in the electrostatics of the Pc−C*f* complex, the effect of ionic strength on the reactivity of alanine single mutants was investigated. As seen in Figure 3, the k_{obs} value for all the mutants with one negative residue replaced with alanine decreased monotonically with an increase in salt concentration in a way similar to that for the C*f*(WT) protein (*21*). Increasing the ionic strength over 0.25 M makes C*f* reduction by PDQ so slow that it impedes a reliable extrapolation of the rate constant at infinite ionic strength (*21*). However, all the alanine single mutants exhibit k_{obs} values similar to that of the C*f*(WT) species at high ionic strengths (ca. 10^3 s^{-1}, Figure 3). These findings indicate that the removal of just one electrostatic charge from the alanine single mutants does not significantly affect the broad negative electrostatic area that interacts with the positive patch of Pc.

The kinetic analysis of the interaction of the two C*f* alanine double mutants, one concerning residues in the small domain and the other concerning residues close to the hydrophobic area of the heme protein, with Pc reveals interesting clues about the involvement of these areas in complex formation and electron transfer. Thus, the double mutant C*f*(D64A/E189A) behaves as the two single alanine mutants (very similar to WT) under standard conditions (Table 1 and Figure 2). This is surprising because the small domain of the Pc−C*f* complex has been proposed to bear the more relevant charged residues involved in the electrostatic interaction with Pc (*17*, *20*, *23*). However, this C*f*(D64A/E189A) mutant yields values much higher than that of C*f*(WT) for k_{obs} at high ionic strengths, as was the case with C*f*(D64K) (Figure 3), suggesting that reducing the negative nature of the small domain (Figure 4) promotes additional effects in the active complex other than purely electrostatics. One possibility, considering the weaker effect of ionic strength, is that in this mutant hydrophobic interactions have a more relevant role in complex formation. Therefore, we can hypothesize that this double mutation may induce a slight change in the structure of the *Nostoc* Pc−C*f* complex from the electrostatically driven side-on configuration to another more similar to the head-on configuration of the *Phormidium* complex, in which the hydrophobic areas of both proteins have a more relevant role in driving productive complex formation (*23*).

With the current data for the C*f*(D100A/E108A) mutant, it is uncertain if this mutant exhibits a dependence of k_{obs} on Pc concentration at low ionic strengths (Figure 2). Whereas the k'_{et} value obtained for this mutant is equivalent to that estimated for the C*f*(D64A/E189A) mutant and only slightly smaller than that for C*f*(WT) (Table 1), the difficulty in obtaining data points at low Pc concentrations (<4 μM), where the extent of C*f* oxidation is very small, prevents the calculation of a reliable value for K_A. However, the dependence profile in Figure 2 may suggest a lower value for this constant with the double mutant compared with the WT, indicating that in such double mutants the electron transfer step is not modified, only the ability of both proteins to encounter each other. Consequently, the dependence of k_{obs} on ionic strength for this mutant leads to values similar to that of C*f*(WT) at high salt concentrations (Figure 3), suggesting that neutralization of these charges is mainly affecting electrostatic interactions. The mutated residues are located in a negative area near the hydrophobic patch of C*f* (Figure 1B), and elimination of these charges markedly diminishes the negative electrostatic potential of this area, making it more hydrophobic (Figure 4), thus altering the interface of the complex in C*f* and affecting short-range forces involved in the formation of the electron transfer complex between C*f* and Pc.

Replacement of single acidic residues with lysine promotes in all cases a decrease in k'_{et} of up to ca. 60% of that with C*f*(WT) without significantly decreasing the values for K_A, as deduced from the independence of k_{obs} from Pc concentration at low ionic strengths [see Figure 2 for the C*f*(E165K)

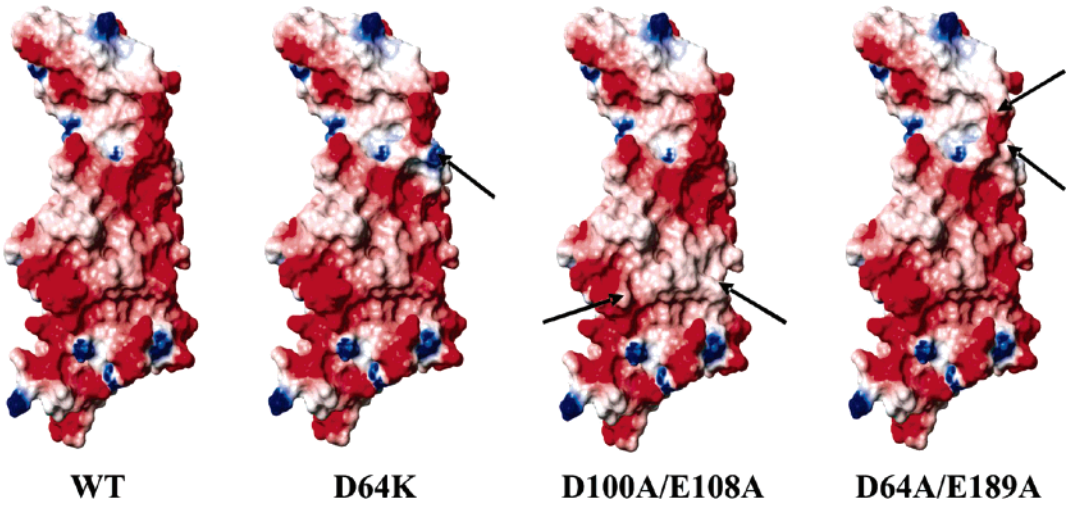

FIGURE 4: Surface electrostatic potential distribution of C*f*(WT) and its D64K, D100A/E108A, and D64A/E189A mutants. In each case, the surface electrostatic potential was estimated at an ionic strength of 200 mM, with 80 and 4 as solvent and protein dielectric constant values, respectively, by using the algorithm by Nicholls and Honig (*29*) and MOLMOL (*30*). Negative and positive potential areas are colored red and blue, respectively. The orientation of the heme protein is the same as in Figure 1A.

mutant, and Table 2]. Thus, whereas a single negative charge removal does not promote drastic kinetic effects, its reversion results in a general decrease in the kinetic efficiency. Such a kinetic effect indicates that the complex formation is driven by the additive result of multiple interactions, which define a broader electrostatic contact area. As was the case with the single alanine mutants, the ionic strength dependence profile of k_{obs} obtained with the single lysine variants indicates a general protein−protein attractive interaction, with k_{obs} approaching C*f*(WT) values at high salt concentrations even though, as expected from the charge substitution, the effect of ionic strength is less pronounced than with WT (see Figure 3 for the E165K variant). The exception to this behavior is that of the C*f*(D64K) mutant, which presents a near independence of k_{obs} with an increase in ionic strength, thereby leading to k_{obs} values higher than that of C*f*(WT) at high ionic strengths (Figure 3). Substitution of this residue, which contributes to the negative electrostatic area of the small domain (Figures 1 and 4), thus promotes additional modifications in the active complex other than purely electrostatics, either by increasing the hydrophobic nature of the interaction forces or by promoting minor modifications in the productive protein−protein orientation or interaction surface.

Cross reactions between mutants of both proteins were carried out to obtain information about specific short-range interactions between charged residues of Pc and C*f*, which can be identified by the reversion of the effects of mutations in these double mutant cross reactions; this approach also could contribute to the definition of the relevance of the different electrostatic areas of C*f* in the interaction with Pc (Tables 1 and 2). The couples of C*f* and Pc mutants to be analyzed by laser flash spectroscopy were selected by taking into account the distance and the relative orientation in the complex of the altered residues (*17*). In most cases, the k_{obs} values for oxidation of C*f* by Pc, as was the case in the WT system, were independent of Pc concentration within the range that was analyzed, except for the cross reaction of the C*f*(D100A/E108A) mutant with the Pc(L14A) mutant (Figure 5 and Table 1). The tentative minimal K_A value obtained for the interaction of the C*f*(D100A/E108A) mutant with the

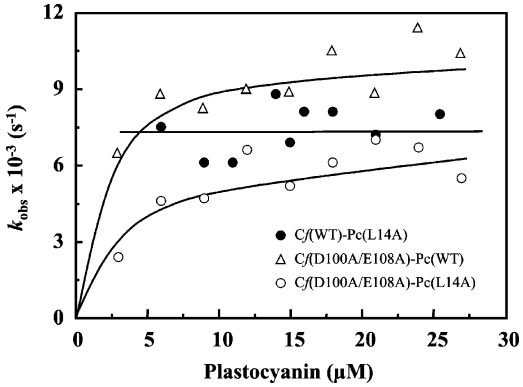

FIGURE 5: Dependence upon Pc concentration of k_{obs} for the oxidation of C*f*(WT) and C*f*(D100A/E108A) by WT and L14A Pc. The lines for the D100A/E108A mutant correspond to the theoretical fittings using the formalism in ref *26*. Experimental data from Albarrán et al. (*21*) with C*f*(WT) and L14A Pc (●) are presented for comparative purposes. Experimental conditions were as described in Experimental Procedures.

Pc(L14A) mutant is lower (ca. 3.4×10^5 M^{-1}) than that of the WT complex (Figure 5 and Table 1). However, the k'_{et} value estimated for this cross reaction is similar to that obtained with C*f*(WT) when it interacts with Pc(L14A) (Table 1). It is also remarkable that the dependence of k_{obs} on Pc concentration previously reported for the interaction of C*f*(WT) with the Pc(K35E) mutant (*21*), a position also involved in formation of the Pc−PSI complex (*22*), disappeared when this Pc mutant interacts with either C*f*(D100K) or C*f*(E108K), the system then recovering the high WT K_A values, although with a decreased k'_{et} (Figure 6 and Table 2), which indicates a restoration of the protein−protein affinity but in a nonoptimal configuration. Taking these results together, we can conclude that there is no strong interaction between any of these charged residues as in any case the WT system behavior was totally recovered (Tables 1 and 2). However, the areas of both proteins in which these residues are located interact very closely in the complex, as deduced from the NMR structure (Figure 1A and ref *17*), and thus, our results suggest that whereas the area defined by D100 and E108 in C*f* is clearly involved in complex formation, the region defined by L14 and K35 in Pc is

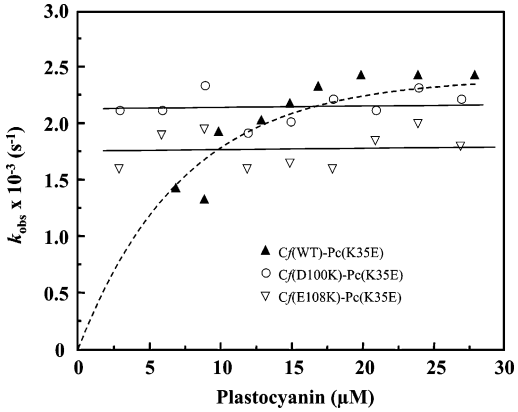

FIGURE 6: Dependence upon Pc concentration of k_{obs} for the oxidation of C*f*(WT), C*f*(D100K), and C*f*(E108K) by K35E Pc. Experimental data from Albarrán et al. (*21*) with C*f*(WT) and K35A Pc (▲) are presented for comparative purposes. The dashed line represents the fitting of experimental data to the equation by Meyer et al. (*26*). Experimental conditions were as described in Experimental Procedures.

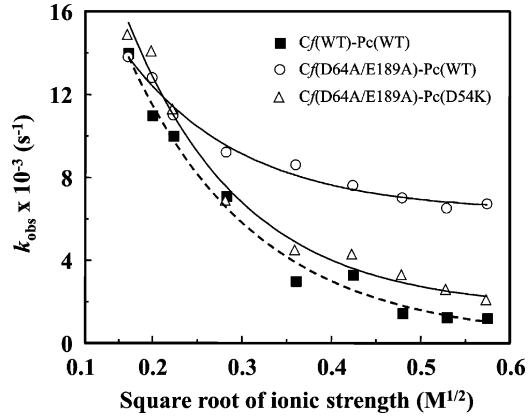

FIGURE 7: Ionic strength dependence of k_{obs} for the interaction of WT Pc and C*f* and for the reaction of C*f*(D64A/E189A) with WT and D54K Pc. The solid and dashed lines represent the fitting of experimental data to the equation by Watkins et al. (*27*). Experimental data from Albarrán et al. (*21*) with C*f*(WT) and Pc (■) are presented for comparative purposes. Experimental conditions were as described in Experimental Procedures.

involved both in the electron transfer step and in the electrostatic interaction for complex formation.

In almost all the reactions between mutants of both proteins, the calculated k'_{et} value is a result of the additive effect of the mutations (Tables 1 and 2). The exception to this rule is the reaction between C*f*(D64K) and Pc(K62E), the k'_{et} being higher than that obtained with the same Pc mutant and C*f*(WT) (Table 2). This result allows us to conclude that the area near the affected residue is close enough in the complex to compensate for the opposite changes of charges on the mutants, in agreement with the structural data of the complex (*17*). Most interesting is the behavior of the reaction between the three C*f* mutants of residue E189 and the Pc(D54K) mutant (Tables 1 and 2), which presents an increased k'_{et} value with C*f*(WT) compared to that with Pc(WT) (*21*). In all these cross reactions, the system recovered the WT k'_{et} value, clearly indicating that these two residues are sufficiently close to each other to reverse the individual effect of the mutation by means of a specific interaction, in particular for the C*f*(E189K) and Pc(D54K) interaction (Table 2). This becomes more evident when the effect of ionic strength on these cross reactions is analyzed. Whereas most of the reactions between mutants of both proteins present the same ionic strength dependences as the reactions of each individual mutant with its respective WT, the reaction between C*f*(D64A/E189A) and Pc(D54K) recovered the WT ionic strength dependence profile (Figure 7), which is not the case when this C*f* mutant interacts with the Pc(K62A) mutant (not shown). Taken together, all these results clearly point to a specific interaction between the area defined by residues D64 and E189 in the small domain of C*f* and the charged D54 residue on Pc. A similar interaction was detected in the plant system (*15*, *28*); however, in the *Phormidium* complex, the equivalent D63 residue in C*f* interacts specifically with R93 in the copper protein (*19*). These results confirm thus the involvement of these areas in the electrostatic nature of the complex, as well as the higher degree of structural similarity of the *Nostoc* complex with the plant system rather than with the other cyanobacterial system (*Phormidium*) analyzed prior to now.

To conclude, our results indicate that a widespread electrostatic area in C*f*, contrary to the more defined surface of Pc, means that replacement of a single charged residue in the heme protein promotes no drastic changes in the interaction with the copper protein. A similar result has been obtained by mutating specific residues in *Phormidium* C*f* (*19*). Thus, there seem not to be key charged residues or "hot spots" in C*f* for the interaction with Pc but an additive effect of multiple specific interactions. We can also conclude that in *Nostoc* C*f* the small domain is the most relevant area in conducting the electrostatic interaction with Pc, so the neutralization of this region turns the nature of the Pc−C*f* complex from electrostatic to more hydrophobic. Moreover, this work makes evident the existence of a specific interaction of residues of the small domain of C*f* with the electrostatic area of Pc.

The different results obtained from analysis of the interaction of C*f*(WT) with site-directed mutants of charged residues in the positive patch of *Nostoc* Pc (*21*), where neutralization or inversion of the charge of key residues promotes significant changes in complex formation and electron transfer, suggest that the electrostatic features of Pc are mainly determining the specificity of the Pc−C*f* interaction.

ACKNOWLEDGMENT

We thank Dr. Antonio Díaz-Quintana for his help in calculating the surface electrostatic potential distributions and Pilar Alcántara for her technical assistance. PDQ and dRf were generous gifts of Prof. Gordon Tollin (University of Arizona, Tucson, AZ).

REFERENCES

1. Hope, A. B. (2000) Electron transfer amongst cytochrome *f*, plastocyanin and photosystem I: Kinetics and mechanisms, *Biochim. Biophys. Acta 1456*, 5−26.
2. Hervás, M., Navarro, J. A., and De La Rosa, M. A. (2003) Electron transfer between soluble proteins and membrane complexes in photosynthesis, *Acc. Chem. Res. 36*, 798−805.
3. De la Rosa, M. A., Molina-Heredia, F. P., Hervás, M., and Navarro, J. A. (2006) Convergent evolution of plastocyanin and cytochrome c_6, in *Photosystem I: The light-driven, plastocyanin:ferredoxin oxidoreductase* (Golbeck, J. H., Ed.) pp 683−696, Springer, New York.
4. Kurisu, G., Zhang, H. M., Smith, J. L., and Cramer, W. A. (2003) Structure of the cytochrome b_6f complex of oxygenic photosynthesis: tuning the cavity, *Science 302*, 1009−1014.

5. Bendall, D. S. (2004) The unfinished story of cytochrome *f*, *Photosynth. Res. 80*, 265−276.
6. Martinez, S. E., Huang, D., Szczepaniak, A., Cramer, W. A., and Smith, J. L. (1994) Crystal structure of chloroplast cytochrome f reveals a novel cytochrome fold and unexpected heme ligation, *Structure 2*, 95−105.
7. Chi, Y. I., Huang, L. S., Zhang, Z. L., Fernandez-Velasco, J. G., and Berry, E. A. (2000) X-ray structure of a truncated form of cytochrome f from *Chlamydomonas reinhardtii*, *Biochemistry 39*, 7689−7701.
8. Gray, J. C. (1992) Cytochrome f: Structure, function and biosynthesis, *Photosynth. Res. 34*, 359−374.
9. Carrell, C. J., Schlarb, B. G., Bendall, D. S., Howe, C. J., Cramer, W. A., and Smith, J. L. (1999) Structure of the soluble domain of cytochrome f from the cyanobacterium *Phormidium laminosum*, *Biochemistry 38*, 9590−9595.
10. Schlarb-Ridley, B. G., Bendall, D. S., and Howe, C. J. (2002) Role of electrostatics in the interaction between cytochrome f and plastocyanin of the cyanobacterium *Phormidium laminosum*, *Biochemistry 41*, 3279−3285.
11. Kannt, A., Young, S., and Bendall, D. S. (1996) The role of acidic residues of plastocyanin in its interaction with cytochrome *f*, *Biochim. Biophys. Acta 1277*, 115−126.
12. Gross, E. L., and Pearson, D. C. (2003) Brownian dynamics simulations of the interaction of *Chlamydomonas* cytochrome *f* with plastocyanin and cytochrome c_6, *Biophys. J. 85*, 2055−2068.
13. Crowley, P. B., Otting, G., Schlarb-Ridley, B. G., Canters, G. W., and Ubbink, M. (2001) Hydrophobic interactions in a cyanobacterial plastocyanin-cytochrome f complex, *J. Am. Chem. Soc. 123*, 10444−10453.
14. Crowley, P. B., and Ubbink, M. (2003) Close encounters of the transient kind: Protein interactions in the photosynthetic redox chain investigated by NMR spectroscopy, *Acc. Chem. Res. 36*, 723−730.
15. Gong, X. S., Wen, J. Q., and Gray, J. C. (2000) The role of amino-acid residues in the hydrophobic patch surrounding the haem group of cytochrome f in the interaction with plastocyanin, *Eur. J. Biochem. 267*, 1732−1742.
16. Ubbink, M., Ejdeback, M., Karlsson, B. G., and Bendall, D. S. (1998) The structure of the complex of plastocyanin and cytochrome f, determined by paramagnetic NMR and restrained rigid-body molecular dynamics, *Structure 6*, 323−335.
17. Díaz-Moreno, I., Díaz-Quintana, A., De la Rosa, M. A., and Ubbink, M. (2005) Structure of the complex between plastocyanin and cytochrome f from the cyanobacterium *Nostoc sp*. PCC 7119 as determined by paramagnetic NMR, *J. Biol. Chem. 280*, 18908−18915.
18. Gross, E. L., and Rosenberg, I. (2006) A Brownian dynamics study of the interaction of *Phormidium* cytochrome *f* with various cyanobacterial plastocyanins, *Biophys. J. 90*, 366−380.
19. Hart, S. E., Schlarb-Ridley, B. G., Delon, C., Bendall, D. S., and Howe, C. J. (2003) Role of charges on cytochrome f from the cyanobacterium *Phormidium laminosum* in its interaction with plastocyanin, *Biochemistry 42*, 4829−4836.
20. Soriano, G. M., Ponamarev, M. V., Piskorowski, R. A., and Cramer, W. A. (1998) Identification of the basic residues of cytochrome f responsible for electrostatic docking interactions with plastocyanin in vitro: Relevance to the electron transfer reaction in vivo, *Biochemistry 37*, 15120−15128.
21. Albarrán, C., Navarro, J. A., Molina-Heredia, F. P., Murdoch, P. S., De la Rosa, M. A., and Hervás, M. (2005) Laser flash-induced kinetic analysis of cytochrome f oxidation by wild-type and mutant plastocyanin from the cyanobacterium *Nostoc* sp. PCC 7119, *Biochemistry 44*, 11601−11607.
22. Molina-Heredia, F. P., Hervás, M., Navarro, J. A., and De la Rosa, M. A. (2001) A single arginyl residue in plastocyanin and in cytochrome c_6 from the cyanobacterium *Anabaena* sp. PCC 7119 is required for efficient reduction of photosystem I, *J. Biol. Chem. 276*, 601−605.
23. Díaz-Moreno, I., Díaz-Quintana, A., De la Rosa, M. A., Crowley, P. B., and Ubbink, M. (2005) Different modes of interaction in cyanobacterial complexes of plastocyanin and cytochrome *f*, *Biochemistry 44*, 3176−3183.
24. Sambrook, J., Fritsch, E. F., and Maniatis, T. (1989) *Molecular Cloning: A Laboratory Manual*, 2nd ed., Cold Spring Harbor Laboratory Press, Plainview, NY.
25. Wells, J. A. (1991) Systematic mutational analysis of protein-protein interfaces, *Methods Enzymol. 202*, 390−411.
26. Meyer, T. E., Zhao, Z. G., Cusanovich, M. A., and Tollin, G. (1993) Transient kinetics of electron transfer from a variety of c-type cytochromes to plastocyanin, *Biochemistry 32*, 4552−4559.
27. Watkins, J. A., Cusanovich, M. A., Meyer, T. E., and Tollin, G. (1994) A "parallel plate" electrostatic model of bimolecular rate constants applied to electron transfer proteins, *Protein Sci. 3*, 2104−2114.
28. Morand, L. Z., Frame, M. K., Colvert, K. K., Johnson, D. A., Krogmann, D. W., and Davis, D. J. (1989) Plastocyanin cytochrome f interaction, *Biochemistry 28*, 8039−8047.
29. Nicholls, A., and Honig, B. (1991) A rapid finite difference algorithm using successive over-relaxation to solve the Poisson-Boltzmann equation, *J. Comput. Chem. 12*, 435−445.
30. Koradi, R., Billeter, M., and Wüthrich, K. (1996) MOLMOL: A program for display and analysis of macromolecular structures, *J. Mol. Graphics 14*, 51−55.

BI0620757